Tensile fracture of heterogeneous solids with distributed breaking strengths

Simon J. D. Cox and Lincoln Paterson
Commonwealth Scientific and Industrial Research Organization, Division of Geomechanics, P.O. Box 54 Mount Waverley, Victoria, Australia 3149
(Received 28 November 1988; revised manuscript received 16 May 1989)

We have used the finite element method in numerical simulations of tensile fracture in an elastic medium with stochastically distributed breaking strengths. We observed that the average number of elements damaged at breakthrough $\langle N \rangle$ on an $L \times L$ square mesh behaves as $\langle N \rangle = \alpha L^{\beta}$. For an exponential distribution of breaking strengths $\alpha \approx 0.3$ and $\beta \approx 2$. For a uniform distribution over $(1-\omega, 1+\omega)$, when $\omega < 0.2$, $\alpha = 1$, and $\beta = 1$. As ω increases above this value, so does β until when $\omega = 1$, $\beta \approx 1.8$. Thus the exponential distribution results in the most disordered and largest damaged area.

INTRODUCTION

The mechanical breakdown of stressed solids is a principal constraint in many areas of science, technology, and engineering. Although heterogeneity is known to prevent ideal behavior in cracks[1] and dislocations,[2] most experimental data and modeling has been either at the phenomenological level or on specific applications with a small number of defects.

When there is a small number of defects, consideration is directed at local perturbations in the general elastic field. This has given rise to the techniques of linear elastic fracture mechanics (LEFM).[3] Attempts have been made to generalize the LEFM treatment of isolated defects by combining components in a micromechanical model,[4] but these approaches tend to be unwieldy with limited intuitive benefit. More recently, work has commenced on elucidating universal principles underlying the breakdown of media which are broadly heterogeneous at the microscopic level.

Models of phase transitions in random systems have shown that for many spatially uncorrelated networks the behavior near to breakdown (the so-called "percolation threshold") can be characterized by a small number of universal exponents.[5] This model of a phase transition from a disordered state with distributed locally transformed sites to an ordered state with a single dominant (connected) strand has proved very rich. Analogs are found in many areas of physics including fluid flow through porous media, electrical breakdown, and fracture. However, in contrast to the simple statistical approaches originally followed in percolation theory, the physics of these other problems demands that account be taken of the local environment of each site, with neighbor-to-neighbor interactions being considered. Furthermore, the contrasts in the nature of the potential field involved in each of these cases may limit the validity of comparisons.

Specifically, there has been some interest in random fuse networks as primitive models for fracture.[6–8] These models consider the variation in a scalar potential (voltage) whereas models of an elastic material must consider tensor fields. A first step in this direction is the network of bars,[9] where the joints are subject to local stresses directed by the links to neighbors. However, to better represent the behavior of continuous media, we need a model which incorporates the full coupling between the components of the stress tensor.

Any general numerical method that solves the stress equations discretizes space and contains an underlying topology. While this may not matter when studying large intact bodies, the underlying structure becomes apparent as the solid becomes diluted via the failure of components during breakdown. Thus the final result may depend heavily on the connectivity of the elements or nodes, which in turn depends on the technique being used. We chose to examine the finite element method because the elements themselves are two-dimensional bodies, unlike the open lattice structure which corresponds to the finite difference approximation. Thus our investigation reveals the consequence of choosing this type of structure and topology.

We have used the finite element method in a Monte Carlo simulation of tensile fracture of a heterogeneous elastic medium. Only one failure mechanism is used, representing the loss of strength of elements in which a critical tensile stress is exceeded. Otherwise the material behaves in a purely elastic manner. In contrast with the similar model by Okubo and Nishimatsu,[10] we have tried not to prejudice our results by accepting a particular model of heterogeneity in advance. Rather, we take an agnostic stance and are testing a number of possibilities in order to determine which factors are most important in controlling the nature of the rupture. In this paper we report on simulations in which the strength distribution is varied within an otherwise homogeneous medium.

It has been observed that the fracture of real materials yields surfaces that are always rough when examined at an appropriate scale, and furthermore, that the fracture of more homogeneous materials produces simpler results than materials with a greater initial heterogeneity.[11] This microstructural distinction is also reflected in measurements of the work done in creating new fracture surfaces. Heterogeneous materials which produce rougher surfaces

and incur more overall damage will absorb more energy in creating the rupture, and are therefore tougher, than similar but homogeneous materials. This has major technological significance particularly for structural ceramics.

NUMERICAL SIMULATIONS

The equations for stress equilibrium in two dimensions are

$$\frac{\partial \sigma_{xx}}{\partial x}+\frac{\partial \sigma_{xy}}{\partial y}=0 ,$$
$$\frac{\partial \sigma_{xy}}{\partial x}+\frac{\partial \sigma_{yy}}{\partial y}=0 . \tag{1}$$

In this paper we study linear elastic solids where the stresses $\{\sigma\}$ and strains $\{\varepsilon\}$ are related by Hooke's law

$$\{\sigma\}=[C]\{\varepsilon\} , \tag{2}$$

where $[C]$ is a constant matrix. For isotropic materials the elastic constants in $[C]$ have only two independent parameters and the constitutive relation in two dimensions for plane stress is

$$\begin{bmatrix}\sigma_{xx}\\ \sigma_{yy}\\ \sigma_{xy}\end{bmatrix}=\frac{E}{1-\nu^2}\begin{bmatrix}1 & \nu & 0\\ \nu & 1 & 0\\ 0 & 0 & (1-\nu)/2\end{bmatrix}\begin{bmatrix}\varepsilon_x\\ \varepsilon_y\\ \gamma_{xy}\end{bmatrix} , \tag{3}$$

where E is the elastic modulus and ν is Poisson's ratio. The plane stress approximation corresponds to a thin plate loaded in the plane. An alternative is to use the constitutive relation for plane strain:

$$\begin{bmatrix}\sigma_{xx}\\ \sigma_{yy}\\ \sigma_{xy}\end{bmatrix}=\frac{E}{(1+\nu)(1-2\nu)}\times\begin{bmatrix}1-\nu & \nu & 0\\ \nu & 1-\nu & 0\\ 0 & 0 & (1-2\nu)/2\end{bmatrix}\begin{bmatrix}\varepsilon_x\\ \varepsilon_y\\ \gamma_{xy}\end{bmatrix} . \tag{4}$$

The plane strain approximation assumes that the geometry and loading do not vary significantly in the longitudinal direction.

The strain compatibility equation in two dimensions is given by

$$\frac{\partial^2 \varepsilon_{yy}}{\partial x^2}+\frac{\partial^2 \varepsilon_{xx}}{\partial y^2}=\frac{\partial^2 \gamma_{xy}}{\partial x \partial y} . \tag{5}$$

Thus, by substituting (3) or (4) into (5) and using (1),

$$\left[\frac{\partial^2}{\partial x^2}+\frac{\partial^2}{\partial y^2}\right](\sigma_{xx}+\sigma_{yy})=0 . \tag{6}$$

For some problems one would attempt to solve (6) directly. However, for the complex geometry that results from a model in which discrete sections are allowed to break, a numerical method is necessary.

The finite element method

Like all numerical approximations, the finite method is based on the principle of discretization. Nevertheless, the technique recognizes the multidimensional continuity of the body. The idealization considers the body as continuous: No separate interpolation process is required to extend the approximate solution to every point within the continuum. The finite element method readily accounts for nonhomogeneity by assigning different properties to different elements. Physically, the finite element concept differs from the lattice analogy in a two-dimensional model (such as the trusses or frames generated by the finite difference approximation) in that the elements themselves are two-dimensional bodies. Continuous elements provide a more natural representation of the properties of the original continuum.

The finite element method relies on two basic assumptions. The first assumption is that transmission of internal forces between the edges of adjacent elements can be represented by interactions at the nodes of the elements. This is done by establishing expressions for nodal forces which are statically equivalent to the forces acting between elements along the respective edges. Thus the procedure seeks to analyze the continuum problem in terms of sets of nodal forces and displacements for the discretized domain.

The other assumption in the finite element method is that displacements are permitted to vary only according to some displacement function prescribed by the user. We chose to use a linear model in which the displacements in a single element (u,v) are related to the coordinates (x,y) by

$$u=\alpha_1+\alpha_2 x+\alpha_3 y$$
$$v=\alpha_4+\alpha_5 x+\alpha_6 y \tag{7}$$

although higher-order terms could have been included, with an infinite number of terms corresponding to the exact solution. This is the key step of finite elements in which a continuum is represented by a piecewise approximation. It also determines the forthcoming matrix $[B]$.

Specific implementation

We chose to use a code based on the source listing in a standard text[12] to determine the stress in each element with either Eq. (3) or (4) for the stress distribution. This code uses quadrilateral elements decomposed into four constant strain triangles. For a constant strain triangle, the strain vector $\{\varepsilon\}$ is related to the nodal displacement vector $\{q\}$ by the relationship

$$\{\varepsilon\}=\frac{1}{2A}\begin{bmatrix} y_2-y_3 & y_3-y_1 & y_1-y_2 & 0 & 0 & 0 \\ 0 & 0 & 0 & x_3-x_2 & x_1-x_3 & x_2-x_1 \\ x_3-x_2 & x_1-x_3 & x_2-x_1 & y_2-y_3 & y_3-y_1 & y_1-y_2 \end{bmatrix}\{q\}=[B]\{q\} , \tag{8}$$

where (x_i,y_i), $i=1,2,3$ are the coordinates of the three nodes of the triangle, A is the area of the triangle, and the nodal displacement vector is given by $\{q\}=(u_1,u_2,u_3,v_1,v_2,v_3)$.

With this definition, a stiffness matrix $[k]$ was calculated for each element

$$[k]=\int\int\int [B]^T[C][B]dV . \tag{9}$$

These individual stiffness matrices where then added together to form a global stiffness matrix $[K]$. The global displacement vector $\{r\}$ was then determined using

$$[K]\{r\}=\{F\} , \tag{10}$$

where $\{F\}$ is the global load vector. Our choice of code uses direct Gaussian elimination with Gauss-Doolittle decomposition of the symmetric stiffness matrix. Strains and stresses in each element were then able to be determined from the nodal displacements.

Evolutionary strategy

Our model gives three components which can be varied: E, ν, and the strength s, as well as a variety of boundary conditions. We chose to follow the lead given by Kahng *et al.*[6] and only consider variations in the strength for a sample in uniaxial tension. We have only used square elements in a square mesh of $L\times L$ elements. For most of the simulations reported here the elements had uniform elastic properties (Poisson's ratio 0.2) but strengths were assigned to each element randomly according to various different probability distributions. Displacements were prescribed for the nodes at the top and bottom of the model to put it into tension, while every other node had a prescribed net load of zero.

After solving for the stress distribution at each step, the mesh is modified to simulate fracture by the following algorithm. The critical element is found, defined as that element in which the ratio of tensile principal stress to element strength is greatest. The element is broken. The stress distribution is recalculated to account for the properties of the changed element, the next critical element broken, and the procedure repeated until the sample fails. Failure is defined as the condition where broken elements connect the two sides of the sample.

In our algorithm, when an element "breaks," the element is not strictly eliminated, but its elastic modulus is reduced to the point where it has no influence on the sequence of broken elements, and its Poisson's ratio is reset to 0.45. Okubo and Nishimatsu[10] determined that a reduction in the elastic constants by a factor of only 100 was sufficient in their simulations, but we found a substantial change between a factor of 100 and 1000 in our simulations. A decrease in the elastic modulus of 4 orders of magnitude was found to be sufficient to meet the criterion, and furthermore, with this change, the difference in the results for plane strain and plane stress became negligible.

The fuse network realizations may be considered equivalent to bond percolation. Our numerical experiments are related to the site percolation problem. However, the coordination of the elements includes two types of bonds to neighbors, at edges and vertices, so our simulations differ from classical site percolation since the elimination of a site still permits its neighbors to be joined at a vertex: Such a joint retains some elastic continuity but does not offer any resistance to rotation. We have not used periodic boundary conditions, unlike some of the studies of resistor networks, because unloaded side boundaries will be more relevant for experimental comparison. However, we have examined the dependence of the results on mesh size L. In an $L\times L$ resistor network, the total number of components which can break is $2L^2$; in a finite element mesh the number is L^2. In both cases the minimum number of failed components required for breakthrough is L.

RESULTS

The geometric results of a simulation can be quantified in a number of ways. Valid estimates of the fractal dimension of the broken surface are difficult because of the limited range of length scales available in practical simulations. We chose rather to follow the percolation model and focus on a "percolation threshold" and cluster size as measures of the degree of irregularity of fracture. In particular, we have measured the number of broken elements N when a broken strand connects the two sides of the mesh and we have examined the behavior of the mean $\langle N\rangle$ as a function of L, $N(L)$, for different strength distributions. In this way we have further improved on Okubo and Nishimatsu's study[10] by including the effect of the model size L on the results.

The strengths of the elements s were assigned randomly according to various probability distributions $f(s)$. Two continuous forms were used, uniform distributions $f(s)=1/2\omega$ over the range $(1-\omega, 1+\omega)$, and a negative exponential distribution $f(s)=e^{-s}$. Samples of the results are shown in Figs. 1 and 2, but each of the results shown in the synoptic figures represents an average over ten simulations with different random number seeds (Figs. 3 and 4).

Uniform distribution of strengths over $(1-\omega, 1+\omega)$

With narrow distributions, the results follow LEFM, with a single strand developing due to the dominance of the stress singularity over the material heterogeneity. In the fuse network analogy where each component has the same conductance (modulus), there is a current (stress)

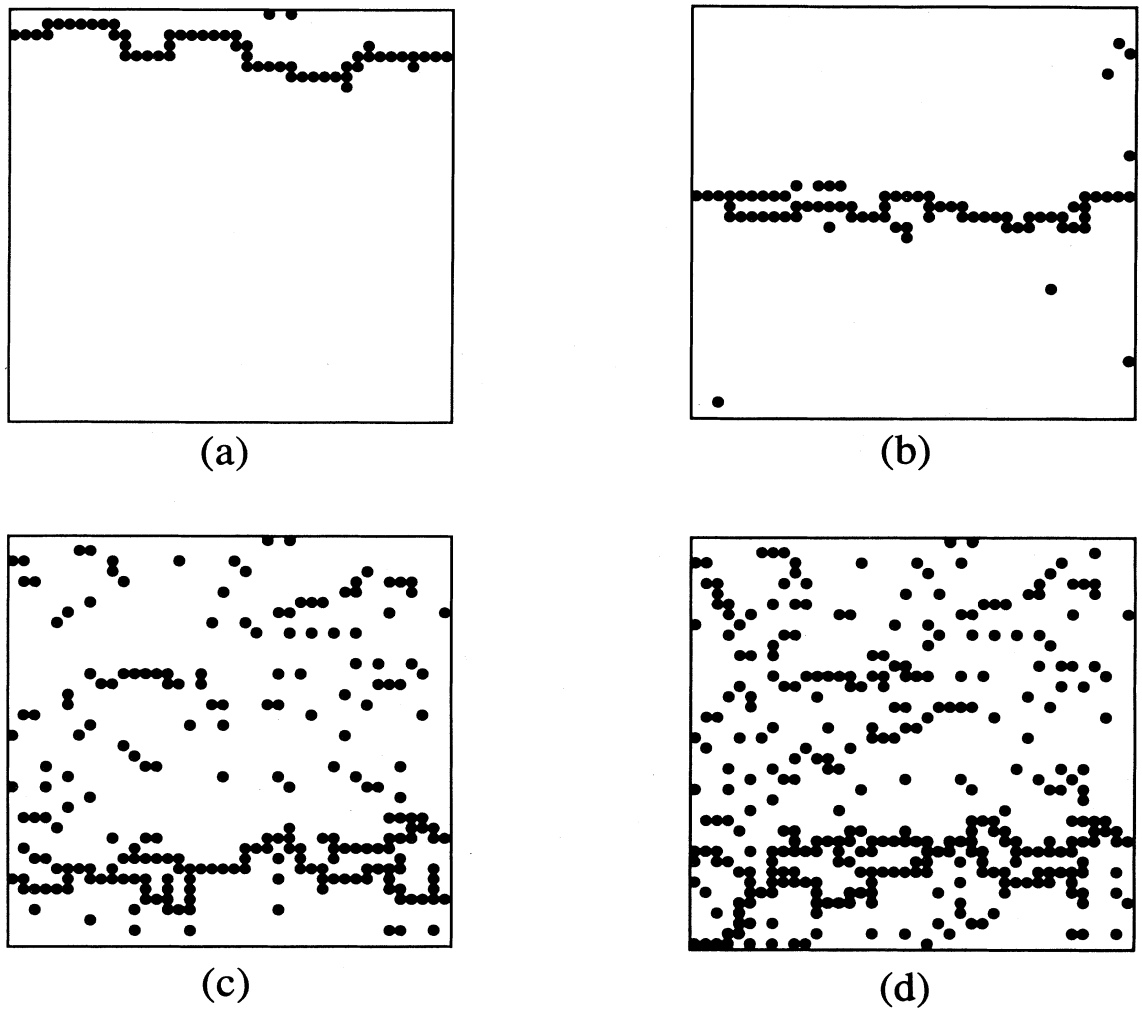

FIG. 1. Some results from simulations on a 40×40 mesh with (a) uniform distribution of strengths with $\omega=0.5$; (b) uniform distribution of strengths with $\omega=0.6$; (c) uniform distribution of strengths with $\omega=0.8$; (d) uniform distribution of strengths with $\omega=1.0$. Broken elements at breakdown are black.

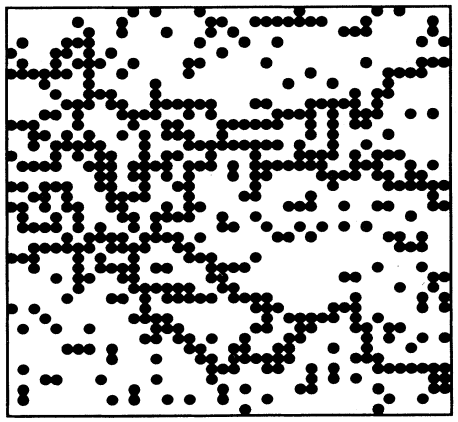

FIG. 2. An example of the result obtained with an exponential distribution of strengths on a 40×40 mesh.

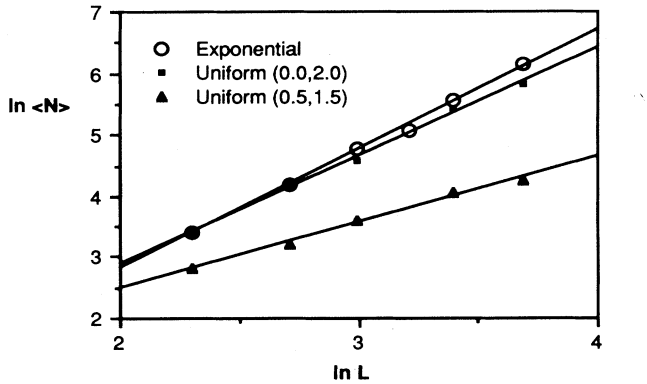

FIG. 3. Variation of the mean number of failed elements at breakthrough $\langle N \rangle$ with the model length L.

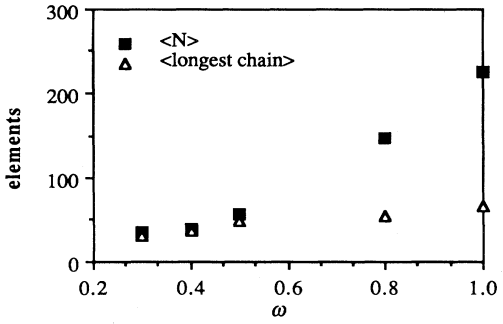

FIG. 4. The total number of failed elements at breakthrough $\langle N \rangle$ and the number of failed elements in the longest chain as a function of ω. This was from a uniform distribution on a 30×30 mesh.

concentration of $4/\pi$ around a single eliminated bond.[8] This result is exact since the Green's function can be solved for the single defect in an infinite medium. For our case, the stress concentration in elements adjacent to a single broken element (defined as the ratio of tensile stress to the mean tensile stress in the mesh) depends on the location of the eliminated element in the mesh. For a Poisson's ratio of 0.2 it was found to be 1.458 for a site in the center of the mesh, independent of the mesh size, and varied between 1.35 and 1.69 for sites elsewhere. For a Poisson's ratio between 0 and 0.4 the stress concentration varies from 1.408 to 1.518 in the center of the mesh. Thus a variation of that factor in the distribution of the breaking strength is required before the fracture path deviates significantly from a straight line.

Our results are summarized in Fig. 3. Kahng *et al.*[6] reported that, in fuse networks, a parameter x defined as $x \equiv \langle N \rangle / L - 1$ appears to grow as a noninteger power of L for large values of ω, with a characteristic exponent that seems to be approaching 1 for values of ω approaching 1. We find similar behavior, except that the exponent of x never reaches 1 (for $\omega = 0.5$, $\langle N \rangle \sim L^{1.1}$; for $\omega = 1.0$, $\langle N \rangle \sim L^{1.8}$). It is trivial to see that an exponent β defined by $\langle N \rangle = \alpha L^{\beta}$ must lie in the range $1 \leq \beta \leq 2$ since values outside this range would predict either $N < L$ or $N > L^2$ as $L \to \infty$. For values of ω above 0.5, most of the additional damage occurs in isolated microfracture away from the main fracture (Fig. 4).

Exponential distribution of strengths

In a study of unstable fluid flow in microstructured porous media[13,14] it was recently found that the most unstable and irregular fluid flow patterns were found in media with an exponential distribution of fluid capacity, which is the most random possible distribution (maximum entropy). We find, analogously, that this distribution of strengths yields the most irregular fracture patterns, with $\langle N \rangle \sim 0.3 L^2$. The amount of damage is thus proportional to the area, or amount of material present initially.

An exponential distribution of strengths is equivalent to breaking each element with a probability proportional to the tensile stress σ in that element. The proof of this argument is identical to the proof given by Chan *et al.*[13] for exponential distributions of fluid capacity. Specifically, for any distribution of strengths $f(s)$,

$$\text{Prob}\{\text{element } i \text{ breaks}\} = \int_0^{\infty} ds_i f(s_i) \times \prod_{\substack{j=1 \\ j \neq i}}^{L^2} \int_{(\sigma_j/\sigma_i)s_j}^{\infty} ds_j f(s_j) \quad (11)$$

is equivalent to

$$\text{Prob}\{\text{element } i \text{ breaks}\} = \sigma_i / \sum_{j=1}^{L^2} \sigma_j \ , \quad (12)$$

providing that $f(s) = a e^{-as}$, where a is an arbitrary constant.

We may compare the exponent $\beta \approx 2$ found in this case with $\beta \approx 1.8$ in the case of the widest possible uniform distribution. A distribution $f(s) = 1/2\omega$, $\omega = 1$ has a variance of 0.5 about a mean value of 1, whereas, with the same normalization, the exponential distribution $f(s) = e^{-s}$ has a variance of 1. Thus, as discussed earlier, the width of the distribution is found to be the dominant control on the irregularity of fracture.

Breaking elements at random

If elements are broken totally at random without regard to their material properties, simulations show that breakthrough from left to right across the sample occurs according to $\langle N \rangle = 0.6 L^2$. This is twice the value for the exponential distribution of strengths. We are unable to offer any explanation for this coincidence.

Exponential distribution of elastic moduli

The bulk of this study has been devoted to distributions of breaking strengths. This is because distributions of elastic moduli have significantly less effect on the results. We include as an example of this observation that the exponential distribution of moduli gives $\langle N \rangle \sim L^{1.54}$.

Mechanical data

The solutions were derived for prescribed displacements of the ends of the model, so the modulus of elasticity for the whole model is simply the ratio of the applied load to this displacement. The applied tensile stress which is required to break the elements in turn is the product of the ratio of strength to stress in the critical element and the model modulus.

In Fig. 5 we plot a typical stress history for a 40×40 model with the exponential strength distribution, with damage statistics shown for correlation. There is a significant drop in the strength after the peak, which corresponds approximately with a coalescence of damage in the model, indicated by a rapid increase in the maximum

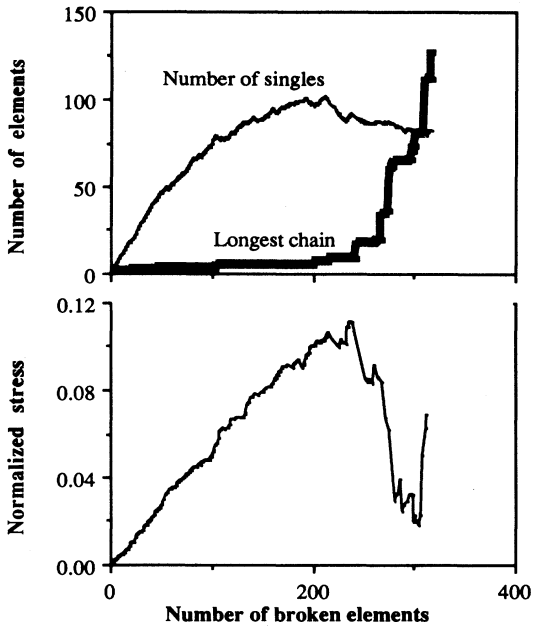

FIG. 5. Number of single broken elements and the number of broken elements in the longest chain as a function of the total number of broken elements. This is for an exponential distribution of strengths on a 40×40 mesh. The stress history is also shown.

cluster size. Although there is a similarity between the curve showing the number of isolated broken elements and the stress history, as shown in Fig. 5 we typically find that the peak in the isolated breaks curve is before the peak stress, after which it levels off rather than decays.

It would be preferable to use a distribution function to examine the correlation of the damage statistics with the load history. However, we found this difficult to do rigorously in models of the size examined here.

CONCLUSIONS

We have examined the breakdown of a square network of elastic elements with a stochastic distribution of the breaking strengths. As the variance of the distribution of strengths increases, so does the average number of broken elements $\langle N \rangle$ at breakthrough. For narrow distributions of strengths, such as the uniform distribution with $\omega < 0.2$, the damaged region forms a straight line with area proportional to L. As ω increases, so does the exponent of L. For the exponential distribution, the damaged area is proportional to the total area, that is $\langle N \rangle \sim L^2$. Thus, of the distributions we tested, the exponential gives the most disordered breakdown. This result has major implications for the design of artificial materials, since it suggests that significant toughening may be achieved with a small proportion of very strong materials bonded into a matrix.

The results presented in this paper required considerably more computational effort than simulations in resistor networks. However, by incorporating the full coupling between strain components, our results serve as a check on the versatility of more primitive models such as resistor networks. Specifically, there appears to be a consistent relationship between $\langle N \rangle$ and L in both our simulations and those of Kahng *et al.* on fuse networks.

[1]A. A. Griffith, Philos. Trans. R. Soc. London Ser. A **221**, 163 (1921).

[2]E. Orowan, Proc. Phys. Soc. **52**, 8 (1940).

[3]B. R. Lawn and T. R. Wilshaw, *Fracture of Brittle Solids* (Cambridge University Press, Cambridge, 1975).

[4]H. Hori and S. Nemat-Nasser, Int. J. Solids Struct. **21**, 731 (1985); A. A. Griffith, in *Proceedings of the First International Congress on Applied Mechanics,* edited by C. B. Biezano and C. B. Burgers (Technische Boekhandel en Drukkerij J. Waltman Jr., Delft, 1924), pp. 55–63.

[5]S. R. Broadbent and J. M. Hammersley, Proc. Cambridge Philos. Soc. **53**, 629 (1954); J. W. Essam, Rep. Prog. Phys. **43**, 833 (1980).

[6]B. Kahng, G. G. Batrouni, S. Redner, L. de Arcangelis, and H. J. Herrmann, Phys. Rev. B **37**, 7625 (1988).

[7]L. de Arcangelis, S. Redner, and H. J. Herrmann, J. Phys. (Paris) Lett. **46**, L585 (1985); A. Gilabert, C. Vanneste, D. Sornette, and E. Guyon, J. Phys. (Paris) **48**, 763 (1987); M. D. Stephens and M. Sahimi, Phys. Rev. B **36**, 8656 (1987).

[8]P. M. Duxbury, P. D. Beale, and P. L. Leath, Phys. Rev. Lett. **57**, 1052 (1986); P. M. Duxbury, P. L. Leath, and P. D. Beale, Phys. Rev. B **36**, 367 (1987).

[9]H. Takayasu, Prog. Theor. Phys. **74**, 1343 (1985); Y. Termonia and P. Meakin, Nature **320**, 429 (1986); L. Paterson, in *Key Questions in Rock Mechanics: Proceedings of the 29th U.S. Symposium,* edited by P. A. Cundall, R. L. Sterling, and A. M. Starfield (Balkema, Rotterdam, 1988), pp. 351–358.

[10]S. Okubo and Y. Nishimatsu, Int. J. Rock Mech. Min. Sci. Geomech. Abstr. **23**, 363 (1986).

[11]S. R. Brown and C. H. Scholz, J. Geophys. Res. **90**, 12575 (1985); S. J. D. Cox and C. H. Scholz, J. Struct. Geol. **10**, 413 (1988).

[12]C. S. Desai and J. F. Abel, *Introduction to the Finite Element Method* (Van Nostrand Reinhold, New York, 1972), Appendix 1.

[13]D. Y. C. Chan, B. D. Hughes, and L. Paterson, Phys. Rev. A **34**, 4079 (1986).

[14]D. Y. C. Chan, B. D. Hughes, L. Paterson, and C. Sirakoff, Phys. Rev. A **38**, 4106 (1988).